

GEOMETRIC INTERPRETATION OF QRS COMPLEXES IN ECG SIGNALS BY RATIONAL FUNCTIONS

Gergő Bognár* and Ferenc Schipp**

(Budapest, Hungary)

Communicated by Sándor Fridli

(Received March 30, 2018; accepted June 25, 2018)

Abstract. In this paper we present a mathematical model for QRS complexes with rational functions. We investigated the geometric properties of the QRS complexes based on this model. Among others, we explored the connection between the fiducial points and parameters of the rational transform, via the roots and the local extrema of the model curve. The importance of this model is twofold. On the first hand, the model provides an analytic way to determine medical descriptors of the QRS complex. On the other hand, it makes possible to synthesize heartbeats from an analytic model that fits the given descriptors.

1. Introduction

The electrocardiogram (ECG) device measures the electric field generated by the heart functioning as the potential between certain points of the body

Key words and phrases: ECG signals, QRS complex, rational functions, heartbeat synthesis
2010 Mathematics Subject Classification: 41A20.

1998 CR Categories and Descriptors: J.3.

*The project has been supported by the European Union, co-financed by the European Social Fund (EFOP-3.6.3-VEKOP-16-2017-00001).

**This research was supported by the Hungarian Scientific Research Funds (OTKA) No K115804.

<https://doi.org/10.71352/ac.47.155>

surface. In the conventional 12-lead ECG, 12 of those potentials are recorded, referred as leads. The signal of each lead can be considered as a quasi-periodic signal consisting of subsequent heartbeats. Normal heartbeats have unique morphology, namely the natural segmentation of them consists of three main waveforms, namely the P and T waves, and the QRS complex. The medical examination process of these waveforms include the determination of the time intervals between the starting and endpoints of the waveforms, such as the QRS duration, the segments and intervals, and the amplitudes, such as the R and S peaks. These starting, end, and peak points are commonly referred as fiducial points. For further information we refer the reader to [6].

Modelling with rational functions have made contributions in ECG processing in several respects [1, 2, 3, 4, 8, 9]. These previous works proved that the adaptive rational transform as a variable projection method is an effective way to model the heartbeats in many respects. In this work, our focus is on the geometric interpretation of the QRS complexes based on the system parameters, the so-called inverse poles, of the rational system, and the coefficients of the projection. To this end, we give a mathematical model in order to locate the roots and the local extrema of the model curve. We provide examples for two possible applications. They are the extraction of the medical descriptors based on the rational model, and the identification of a model that fits to a given set of descriptors. We discuss multiple use cases for the latter one.

2. The mathematical model

We utilize the rational functions to model ECG heartbeats. The rational functions can be expressed as linear combination of the (normalized) basic rational functions:

$$r_a(z) := \frac{1 - |a|}{1 - \bar{a}z}, \quad r_{a,n}(z) = r_a^n(z) \quad (z \in \mathbb{C}, a \in \mathbb{D}, n \in \mathbb{N}).$$

Here, the parameter $a = \rho e^{i\alpha}$ is the so-called inverse pole which is the inverse of the pole $a^* = 1/\bar{a}$, and n is referred to as multiplicity. We note that the term normalized is used in the sense of the range: $\max_{t \in \mathbb{R}} |r_\rho(e^{it})| = 1$. We consider the restriction of these functions to the unit circle or torus \mathbb{T} , i.e. $r_{a,n}(e^{it})$ ($t \in \mathbb{R}$) which is periodic by 2π . In the previous works the heartbeats were approximated with the superposition of the basic rational functions. It was based on the observation that the graphs of the real and imaginary parts of these functions along with the linear combination of them, are similar to the ECG waveforms on the leads. More precisely, if we consider $N \in \mathbb{N}$ inverse

poles $a_j \in \mathbb{D}$ with multiplicities $m_j \in \mathbb{N}$ ($j = 1, \dots, N$), then the ECG signal can be expressed with the real coefficients u and v :

$$\begin{aligned} E(t) &:= \sum_{j=1}^N \sum_{k=1}^{m_j} \Re(r_{a,k}(e^{it}))u_{j,k} + \sum_{j=1}^N \sum_{k=1}^{m_j} \Im(r_{a,k}(e^{it}))v_{j,k} = \\ &= \Re \left(\sum_{j=1}^N \sum_{k=1}^{m_j} (u_{j,k} - iv_{j,k})r_{a,k}(e^{it}) \right) \quad (t \in \mathbb{R}). \end{aligned}$$

For modelling QRS complex we propose to involve only one inverse pole $a \in \mathbb{D}$ with multiplicity $n \in \mathbb{N}$. Normalizing the coefficient, we obtain the following form expressed with the coefficient parameter $\theta \in [-\pi, \pi]$:

$$(2.1) \quad E_\theta(t) := \Re(e^{-i\theta}r_a^n(e^{it})) = \Re(r_a^n(e^{it}))\cos\theta + \Im(r_a^n(e^{it}))\sin\theta \quad (t \in \mathbb{R}).$$

Recall that the Blaschke function with an inverse pole $a = \rho e^{i\alpha} \in \mathbb{D}$ is of the form

$$B_a(e^{it}) := \frac{e^{it} - a}{1 - \bar{a}e^{it}} = e^{i\alpha}B_\rho(e^{i(t-\alpha)}) = e^{i\alpha}e^{i\gamma_\rho(t-\alpha)} \quad (t \in \mathbb{R}),$$

where

$$\gamma_\rho(t) := 2 \arctan \left(\sigma(\rho) \tan \left(\frac{t}{2} \right) \right) \quad (t \in \mathbb{R}), \quad \left(\sigma(\rho) := \frac{1+\rho}{1-\rho} \right).$$

Then the function $r_\rho(e^{it})$ can be expressed in polar coordinates as

$$r_\rho(e^{it}) = R_\rho(t)e^{i\omega_\rho(t)} \quad (t \in \mathbb{R}),$$

where the magnitude and argument functions are given by

$$\omega_\rho(t) := \frac{\gamma_\rho(t) - t}{2}, \quad R_\rho(t) := \frac{|1 - \rho|}{|1 - \rho e^{it}|} \quad (t \in \mathbb{R}).$$

We remark that both of the magnitude and argument functions can be expressed by the well-known Poisson-kernel. Namely

$$R_\rho(t) = \sigma_\rho^{-1/2} P_\rho^{1/2}(t), \quad \gamma_\rho(t) = \int_0^t P_\rho(\tau) d\tau,$$

where P_ρ is the Poisson kernel:

$$P_\rho(t) := \frac{1 - \rho^2}{1 - 2\rho \cos t + \rho^2} \quad (t \in \mathbb{R}).$$

We also note that the parametric function family γ_ρ ($\rho \in (-1, 1)$) is closed under the operation of function composition. In particular, the inverse of γ_ρ is $\gamma_{-\rho}$.

The model function E_θ can now be expressed in an explicit form as

$$(2.2) \quad \begin{aligned} E_\theta(t) &= \Re(e^{-i\theta} r_a^n(e^{it})) = \Re(e^{-i\theta} r_\rho^n(e^{i\tau})) = \Re\left(R_\rho(t)^n e^{i(n\omega_\rho(\tau) - \theta)}\right) = \\ &= R_\rho(t)^n \cos(n\omega_\rho(\tau) - \theta) \quad (\tau := t - \alpha). \end{aligned}$$

We call the attention the symmetric and antisymmetric behaviour of the cases $\theta = 0$ and $\theta = \pi/2$, illustrated in Fig. 1. In these two cases, the model functions are actually the real and imaginary parts of the corresponding basic rational function over the torus, while in every other case (i.e. for other values of θ), the model function is a proper linear combination of them.

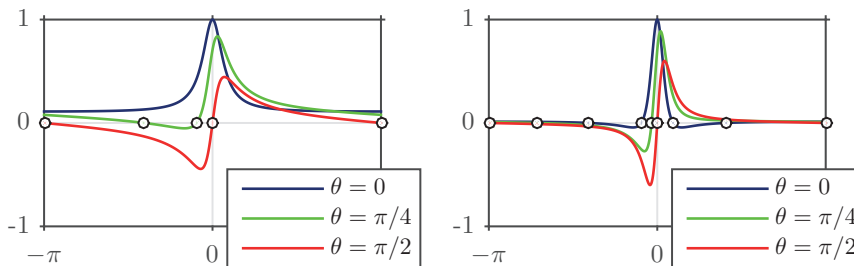


Figure 1. Examples of the model function E_θ for multiplicities $n = 1$ (left) and $n = 2$ (right), with inverse pole $a = 0.8$.

3. Fiducial point extraction

Based on the model above, we have an analytical way to describe the QRS complex. In this section we focus on the locations of the roots and local extrema. The motivation behind this is that the roots, as the baseline crossings are expected to be in connection with the starting and end points, and the local extrema with the peaks of the QRS complex. This means that these medical descriptors of QRS complexes can be extracted directly from the model.

3.1. Roots

By (2.2), we have the following equations for the roots of E_θ :

$$(3.1) \quad n\omega_\rho(\tau) - \theta = \frac{\pi}{2} - k\pi \iff \omega_\rho(\tau) = \frac{2\theta - (2k-1)\pi}{2n} =: \xi_k \quad (k \in \mathbb{Z}).$$

Each equation in (3.1) has at most two non-necessarily distinct roots in the interval $[-\pi, \pi)$. The number of the roots depend on the relationship between the range of ω_ρ and ξ_k 's. Namely, the function ω_ρ has local minimum and maximum points at some $\pm\tau_0$ (for which $\cos\tau_0 = \rho$), thus its range is the interval between $\pm\omega_\rho(\tau_0)$. In general, we conclude that E_θ has up to $2n$ roots in $[-\pi, \pi)$.

In Fig. 2 the function ω_ρ and the roots of the equations $\omega_\rho(\tau) = \xi_1$ are presented for $n = 2$ with some coefficient parameters. We note that in case of $n = 2$, assuming that $\theta \geq 0$, we have two possible equations to solve:

$$\omega_\rho(\tau) = \xi_1 = \frac{\theta - \pi/2}{2}, \quad \omega_\rho(\tau) = \xi_2 = \frac{\theta - 3\pi/2}{2}.$$

The results of the first one are visualized in Fig. 2. We also refer to Fig. 1, where the roots are highlighted on the model functions, as well.

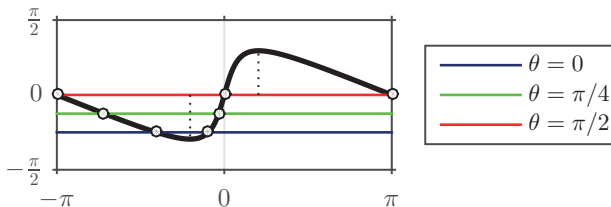


Figure 2. The function ω_ρ , and the roots of $\omega_\rho(\tau) = \xi_1$ (depending on θ), for $n = 2$ and $\rho = 0.8$.

3.2. Local extrema

At first we consider the derivatives of the basic rational functions:

$$\frac{d}{d\tau} r_\rho^n(e^{i\tau}) = \frac{in\rho e^{i\tau}}{1-\rho} r_\rho^{n+1}(e^{i\tau}) = \frac{n\rho R_\rho^{n+1}(\tau)}{1-\rho} e^{i((n+1)\omega_\rho(\tau) + \tau + \pi/2)}.$$

Thus, the derivative E'_θ has a form similar to (2.2):

$$E'_\theta(t) = \Re \left(e^{-i\theta} \frac{d}{d\tau} r_\rho^n(e^{it}) \right) = \frac{n\rho R_\rho^{n+1}(\tau)}{1-\rho} \Re \left(e^{i((n+1)\omega_\rho(\tau) + \tau + \pi/2 - \theta)} \right) =$$

$$= \frac{n\rho R_\rho^{n+1}(\tau)}{1-\rho} \cos((n+1)\omega_\rho(\tau) + \tau + \pi/2 - \theta).$$

Then we have the following equations for the critical points:

$$(3.2) \quad (n+1)\omega_\rho(\tau) + \tau + \frac{\pi}{2} - \theta = \frac{\pi}{2} + k\pi \iff$$

$$\iff \omega_\rho(\tau) = -\frac{\tau}{n+1} + \frac{\theta + k\pi}{n+1} =: -\frac{\tau}{n+1} + \xi_k \quad (k \in \mathbb{Z}).$$

The discussion on the number of the solutions is similar to that of the previous subsection. Each equation of (3.2) has at most two non-necessarily distinct roots in the interval $[-\pi, \pi)$. The number of the roots depends on the relationship between ξ_k 's and the range of $\omega_\rho^*(\tau) := \omega_\rho(\tau) + \tau/(n+1)$. Namely, if $\rho \in (0, 1/n]$ then the function ω_ρ^* is strictly increasing, while if $\rho \in (1/n, 1)$ then ω_ρ^* has local minimum and maximum points at some $\pm\tau_0$. Thus, its range is the interval between $\pm\pi/(n+1)$ in the first, and $\pm\omega_\rho^*(\tau_0)$ in the second case. In general, we conclude that E'_θ have up to $2n+2$ roots on $[-\pi, \pi)$.

If the inverse pole a and the coefficient parameter θ are fixed, then the numerical approximation of the solutions of (3.2) is advised. For instance, by the application of the bisection method multiple times on intervals derived from the roots of E_θ .

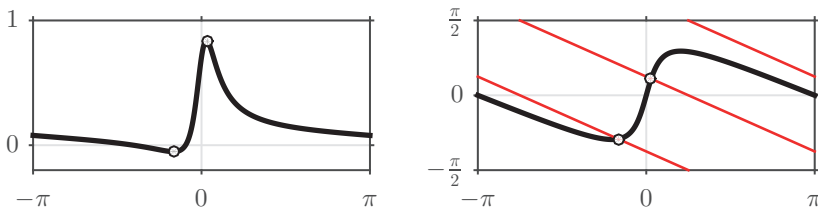


Figure 3. The local extrema of the model function E_θ , and the roots of equation (3.2), for $n = 1$, with $\theta = \pi/4$, and $\rho = 0.8$.

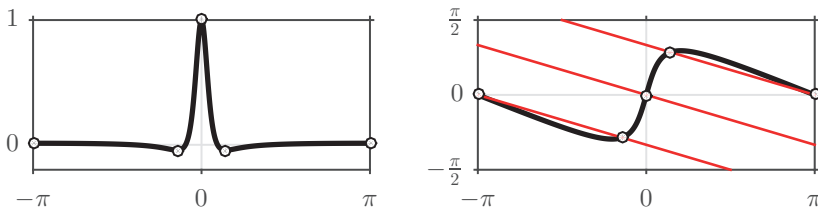


Figure 4. The local extrema of the model function E_θ , and the roots of equation (3.2), for $n = 2$, with $\theta = 0$, and $\rho = 0.8$.

4. Parameter reconstruction based on medical descriptors

In this section we consider the inverse problem, i.e. the identification of the parameters of the model function E_θ of (2.1), based on the given medical descriptors of the QRS complex. This technique can lead to heartbeat synthesis methods, where we can generate artificial heartbeats from an analytic model that fits the given descriptors.

In the following subsection we investigate three possible cases, where the parameters of the model function are reconstructed based on the local minimum and maximum points of the QRS curve. These minimum and maximum points correspond to the locations of the Q, R, and S peaks. These are also related to other common medical descriptors, such as the ventricular activation time (VAT), or the QRS duration. We note, that we use only the local extrema points instead of the roots, because of the uncertainty of the zero level of the heartbeats in practice. In the example cases, we assumed different restrictions about the model curve: even, odd, or the magnitude of the inverse pole is fixed. The multiplicity of the model function is set to $n = 2$, based on the previous experiences on the behaviour of the QRS complex [4].

We remark that as system identification techniques, these methods represent a different approach comparing to the various optimization methods, such as the Hyperbolic Nelder–Mead method [4], the Hyperbolic Particle Swarm Optimization (HPSO) [8], or the gradient Variable Projection methods [9], that have already been applied for ECG heartbeats to identify the best fitting rational system. Namely, this approach is meant to ensure that the heartbeats and their rational projection have the same medical descriptors, even at the expense of the approximation error.

4.1. Symmetric (even) case

In this case we assume that $\theta = 0$, i.e. the model function E_θ is symmetric. Let the line of symmetry be the axis Y, i.e. the complex argument of the inverse pole is $\alpha = 0$, which also means that the location of the R peak is selected to be $t_0 = 0$. The input information of this case are the local minimum points t_1 and $t_2 = -t_1$ of E_0 , that may correspond to the locations of the Q and S peaks (see Fig. 5). The only parameter to be reconstructed is the complex magnitude ρ of the inverse pole. From (3.2) we have the following (with $k = 1$):

$$\frac{\gamma_\rho(t_2) - t_2}{2} = \omega_\rho(t_2) = -\frac{t_2}{3} + \frac{\pi}{3} \iff 2 \arctan \left(\sigma(\rho) \tan \left(\frac{t_2}{2} \right) \right) = \frac{t_2}{3} + \frac{2\pi}{3},$$

from where ρ can be determined from a given t_2 :

$$\sigma_0 := \sigma(\rho) = \frac{1 + \rho}{1 - \rho} = \frac{\tan(t_2/6 + \pi/3)}{\tan(t_2/2)} \iff \rho = \frac{\sigma_0 - 1}{\sigma_0 + 1}.$$

We note that, assuming that $t_2 > 0$ (more precisely $t_2 \in (0, \pi)$), we have to choose $k = 1$ in (3.2) (or in general $k = 1 + 3m$ ($m \in \mathbb{Z}$)) in order to ensure that the reconstructed inverse pole is within the unit disk.

4.2. Antisymmetric (odd) case

In this case we assume that $\theta = \pi/2$, i.e. the model function E_θ is antisymmetric. Similarly to the previous case, let the point of symmetry be the origin, i.e. the complex argument of the inverse pole is $\alpha = 0$. The input information are the local minimum point t_1 and the local maximum point $t_2 = -t_1$ of $E_{\pi/2}$, that may correspond to the locations of the Q (or S) and the R peaks, respectively (see Fig. 5). The only parameter to be reconstructed is ρ , again. From (3.2) we have the following (with $k = 0$):

$$\frac{\gamma_\rho(t_2) - t_2}{2} = \omega_\rho(t_2) = -\frac{t_2}{3} + \frac{\pi}{6} \iff 2 \arctan \left(\sigma(\rho) \tan \left(\frac{t_2}{2} \right) \right) = \frac{t_2}{3} + \frac{\pi}{3},$$

from where ρ can be determined from a given t_2 :

$$\sigma_0 := \sigma(\rho) = \frac{1 + \rho}{1 - \rho} = \frac{\tan(t_2/6 + \pi/6)}{\tan(t_2/2)} \iff \rho = \frac{\sigma_0 - 1}{\sigma_0 + 1}.$$

We note, that as oppose to the previous case, now we have to choose $k = 0$ in (3.2) (or in general $k = 3m$ ($m \in \mathbb{Z}$)), to get an inverse pole within the unit disk. In addition to that, now we need $t_2 < \pi/2$ as well (assuming that $t_2 > 0$).

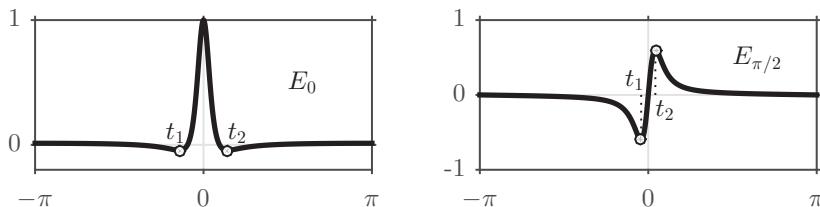


Figure 5. Parameter reconstruction for the symmetric (even) and antisymmetric (odd) cases: $\theta = 0$ and $\pi/2$.

4.3. General case

In this case we assume that the complex magnitude ρ of the inverse pole is known. Besides that, the input information, similarly to the antisymmetric case, are the local minimum point t_1 and the local maximum point t_2 (see Fig. 6). The parameters to be reconstructed are the complex argument α of the inverse pole, and the coefficient parameter θ . From (3.2) we have the following equations for $j = 1, 2$ (with the corresponding $k = \pm 1, 0$):

$$\frac{\gamma_\rho(\tau_j) - \tau_j}{2} = -\frac{\tau_j}{3} + \frac{\theta}{3} + \xi_j \iff 2 \arctan\left(\sigma(\rho) \tan\left(\frac{\tau_j}{2}\right)\right) = \frac{\tau_j}{3} + \frac{2\theta}{3} + 2\xi_j,$$

where $\tau_j = t_j - \alpha$ ($j = 1, 2$), $\xi_1 = \pm\pi/3$, and $\xi_2 = 0$. We note that the sign in k and ξ_1 depend on whether the local minimum points precedes (-1) or follows the maximum point ($+1$). Set $\sigma := \sigma(\rho)$, and $T_j := \tan(\tau_j/2)$ ($j = 1, 2$). Then the equations take the form

$$(4.1) \quad \arctan(\sigma T_j) = \frac{\arctan(T_j)}{3} + \frac{\theta}{3} + \xi_j \quad (j = 1, 2).$$

The subtraction of the equations (4.1) leads to

$$(4.2) \quad \arctan(\sigma T_2) - \arctan(\sigma T_1) = \frac{t_2 - t_1}{6} + \xi_2 - \xi_1.$$

Let $t_0 := t_2 - t_1$, $\xi_0 = \xi_2 - \xi_1$. Apply the trigonometric addition formulas of \tan to (4.2), and to the line $t_0/2 = \tau_2 - \tau_1 = \arctan(T_2) - \arctan(T_1)$ to obtain

$$(4.3) \quad \begin{aligned} \frac{\sigma(T_2 - T_1)}{1 + \sigma^2 T_1 T_2} &= \tan\left(\frac{t_0}{6} + \xi_0\right), \\ \frac{T_2 - T_1}{1 + T_1 T_2} &= \tan\left(\frac{t_0}{2}\right). \end{aligned}$$

Dividing the equations (4.3) we have

$$\frac{1 + T_1 T_2}{1 + \sigma^2 T_1 T_2} = \frac{\tan(t_0/6 + \xi_0)}{\sigma \tan(t_0/2)} =: \sigma_0 \iff T_1 T_2 = \frac{1 - \sigma_0}{\sigma_0 \sigma^2 - 1} := \kappa_1.$$

Substituting that into (4.3) we get

$$T_2 - T_1 = \tan\left(\frac{t_0}{2}\right) (1 + \kappa_1) := \kappa_2,$$

from where T_1 and T_2 can be computed. Then the parameter θ can be reconstructed from (4.1), and the parameter α from the line $\arctan(T_1) = (t_1 - \alpha)/2$.

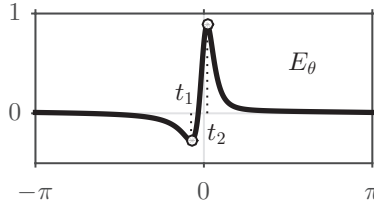


Figure 6. Parameter reconstruction for general case, with $\rho = 0.8$.

5. Evaluation on real ECG heartbeats

We evaluated the proposed antisymmetric, and the general case parameter reconstruction methods on some selected records from the MIT-BIH Arrhythmia Database [10], available on PhysioNet [5]. This database is the most widely used annotated test dataset on the field of ECG signal processing, consisting of more than 100 000 heartbeats. For the evaluation, we split the selected records into heartbeats, based on the database annotations, and we applied the methods for each heartbeats independently. The preprocessing and the segmentation of the heartbeats were performed as in our previous study [1].

The antisymmetric reconstruction method was evaluated on the second lead (V1) of record #112, for 2536 normal (non-arrhythmic) heartbeats (which can be assumed antisymmetric). At first, according to the local minimum and maximum points, we reconstructed the parameters of E_θ for each heartbeat, based on the proposed antisymmetric method above. At second, we computed the parameters of the best fitting model function by means of the local L_2 error calculated over the neighborhood of the local extrema points. We performed a Hyperbolic Nelder–Mead optimization method for this task. Then we calculated the PRDs (percent root-mean-square differences) between the model functions and the corresponding heartbeats. The quantitative analysis on the PRDs shows that the model functions derived from the reconstruction method have worse approximation properties than the best fitting model, but only with a factor of 2. Namely, the mean and standard deviation of the PRDs for the reconstructed model are 50% and 11%, compared to the 24% and 5% of the fitted model. The pairwise comparison gives the same result, the ratio of the PRDs of the two models is 2.2 on average. We note that, as Fig. 7 demonstrates, the signal-to-noise ration of this record is high, even after the usual preprocessing, thus the PRDs of these sizes are expected and acceptable.

The general reconstruction method was evaluated on the first lead (MLII) of record #104 and #105, for 2589 normal heartbeats, with similar methodology as above. In the general case we assumed that the parameter ρ , the

magnitude of the inverse pole, is known, and then the other parameters can be reconstructed according to the local extrema points. In this evaluation, we performed a one-dimension Nelder–Mead optimization method for the parameter ρ , in the reconstruction method, as well. The quantitative analysis shows a more promising result now, the reconstructed model and the best fitting model have similar approximation properties. Namely, the mean and standard deviation of the PRDs for the reconstructed model are now 18% and 12%, compared to the 9% and 5% of the fitted model. The ratio of the PRDs of the two models is 1.5 on average.

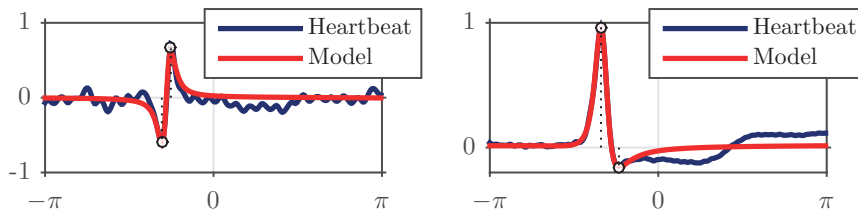


Figure 7. Sample heartbeats and the reconstructed model functions, from the records #112 and #104. We note, that our model is restricted only to the QRS complex of the heartbeats, the model function is expected to approximate only that part of the heartbeat.

According to the evaluation of the selected portion of the database, we can conclude that the model function E_θ , and the proposed reconstruction methods can be utilized in a real environment, as well. For the selected heartbeats, the reconstructed model of the general case is nearly as good approximator as the best one possible, while we can guarantee that the reconstructed model and the original heartbeat agree on the selected fiducial points, considered as medical descriptors.

6. Future work

Our future plans include a more detailed, further evaluation of the model on ECG databases, the extension of the model to P and T waves as well, and the development of a reliable fiducial point detector and a realistic heartbeat synthesiser.

References

- [1] **Bognár, G. and S. Fridli**, Heartbeat classification of ECG signals using rational function systems, in: R. Moreno Díaz et al. (Eds.) *Proc. 16th EUROCAST 2017, Part II*, LNCS **10672**, Springer, 2018, 187–195.
- [2] **Fridli, S. and F. Schipp**, Biorthogonal systems to rational functions, *Ann. Univ. Sci. Budapest., Sect. Comp.*, **35** (2011), 95–105.
- [3] **Fridli, S., L. Lócsi and F. Schipp**, Rational function system in ECG processing, in: R. Moreno Díaz et al. (Eds.) *Proc. 13th EUROCAST 2011, Part I*, LNCS **6927**, Springer, 2012, 88–95.
- [4] **Fridli, S., P. Kovács, L. Lócsi and F. Schipp**, Rational modeling of multi-lead QRS complexes in ECG signals, *Ann. Univ. Sci. Budapest., Sect. Comp.*, **37** (2012), 145–155.
- [5] **Goldberger., A.L., et al.**, PhysioBank, PhysioToolkit, and PhysioNet: Components of a new research resource for complex physiologic signals, *Circulation*, **101**, 23 (2000), e215–e220,
<http://circ.ahajournals.org/content/101/23/e215>
- [6] **Goldberger., A.L.**, *Clinical Electrocardiography: a Simplified Approach*, (7nd), Mosby Elsevier, Philadelphia, 2006.
- [7] **Kovács, P. and L. Lócsi**, RAIT: the Rational Approximation and Interpolation Toolbox for Matlab, with Experiments on ECG Signals, *Int. J. Adv. Telecom. Elect. Sign. Syst.*, **1** (2012), 67–75.
- [8] **Kovács, P., S. Kiranyaz and M. Gabbouj**, Hyperbolic particle swarm optimization with application in rational identification, in: *Proc. 21st Euro. Sign. Proc. Conf.*, 2013, 1–5.
- [9] **Kovács, P.**, Rational variable projection methods in ECG signal processing, in: R. Moreno Díaz et al. (Eds.) *Proc. 16th EUROCAST 2017, Part II*, LNCS **10672**, Springer, 2018, 196–203.
- [10] **Moody, G.B. and Mark, R.G.**, The Impact of the MIT-BIH Arrhythmia Database, *IEEE Eng. Med. Biol. Mag.*, **20**, 3 (2000), 45–50.

G. Bognár and F. Schipp

Department of Numerical Analysis

Faculty of Informatics

ELTE Eötvös Loránd University

H-1117 Budapest, Pázmány P. sétány 1/C

Hungary

bognargergo@caesar.elte.hu

schipp@numanal.inf.elte.hu